ISSN 1392−1207. MECHANIKA. 2017 Volume 23(2): 253−258

Effects of thermal loading on the deployment of four-bar linkages for retractable roof structures

Jianguo Cai*, Xiaowei Deng, Yaozong Zhao***, Jian Feng******

**Key Laboratory of C & PC Structures of Ministry of Education, Southeast University, Nanjing 210096, China, E-mail: j.cai@seu.edu.cn*

***Department of Civil Engineering, University of Hong Kong, Hong Kong, China, E-mail: xwdeng@hku.hk*

**** School of Civil Engineering, Southeast University, Nanjing 210096, China, E-mail: 230079101@seu.edu.cn*

*****National Prestress Engineering Research Center, Southeast University, Nanjing 210096, China, E-mail: fengjian@seu.edu.cn*

crossref http://dx.doi.org/10.5755/j01.mech.23.2.12542

1. Introduction

Deployable structure, which is a structure that can change its size by changing its shape, is widely used in daily life such as tents and umbrellas. Current interest in deployable structures arises mainly from their potential in space engineering, civil engineering and MEMS [1-3].The deployment analysis is an important part in the theoretical research and design of deployable structures.

There are some methods developed for flexible multibody dynamic analysis. The classical method of kinematics and dynamics of flexible multibody systems are described in many textbooks on multibody dynamics [4-6]. Moreover, it is implemented in some commercial software such as ADAMS and DADS. These methods are obtained with extending the methodology for rigid system by assuming that the global motion of structural members is composed of a rigid body motion and a small deformation [4, 7, 8]. The main limitation of these methods is that structural members should be linear elasticity in the rigid body frame, which leads to the nonlinear effects such as geometric stiffening cannot be considered.

Another general and versatile approach in flexible multibody dynamics is the Finite Element method. In this method, the description of large displacements and rotations requires a nonlinear geometric formulation [9, 10]. In order to circumvent the difficult treatment of rotations, Shabana [11] proposed the Absolute Nodal Coordinate Formulation, where the location and deformation of a material point in the finite element are defined in the global coordinate system. This leads to great convenience for solving efficiently the dynamic equation of system [12]. The beam and shell element formulations of this method have been studied by many researchers [13-18]. However, the temperature field was not considered in most of these researches and all the analyzed mechanical systems work under the normal temperature. There are larger temperature changes for the work environment of deployable structures. The constraint forces and the internal forces of structural members will increase due to thermal stress with the raise of the temperature, which may leads to the failure of the deployment of deployable structures. Therefore, Li and Wang [19] investigated the flexible body dynamics of deployable structures under different temperatures using the absolute nodal coordinate formulation. They found that the influence factors of deployment dynamic characteristics include the structural form, material properties, geometric parameters and deployment planning in ambient and thermal/vacuum environments.

On the other hand, Géradin and Cardona [20] proposed a systematic methodology for mechanisms analysis using the advanced Finite Element method. They presented a full departure from traditional approaches in the sense that the total motion, which consists of rigid body motion and elastic deformation, is directly refereed to the inertial frame. Therefore, elastic effects are naturally introduced in the model. The stiffness properties of each elastic member can be described in a quite rigorous manner, including the geometric stiffening effects. Moreover, the topology of the structure is implicitly contained in the finite element mesh, which avoiding the need for a description of complex closed loop systems based on graph theory [20-22].

Normally, it is necessary to use a computer to simulate the kinematics and dynamics of the flexible system. The existing commercial software such as ADAMS and DADs can simulate the rigid and flexible multibody dynamics of mechanical systems, but the structural analysis cannot be considered [19]. In this paper, a method is presented for the flexible multibody dynamic analysis of deployment of deployable structures under the temperature field. The finite element method originally proposed in [20] by Géradin and Cardona is employed here. The paper is organized as follows: Section 2 gives the general formulation of the dynamics of a multibody system. Following by the dynamic equations considering thermal effects are given in Section 3. Then two numerical examples are carried out in Section 4 to study the influence of thermal loading on the behavior during the motion. Conclusions are given in Section 5.

2. General formulation of the dynamics of a multibody system

It is very convenient to express the dynamic equations of a multibody system in terms of finite element coordinates [20-22]. Therefore, this section will briefly introduce the kinematic and dynamics of a bar system with the method proposed by Géradin and Cardona [20].

The axial strain components of bars are given with the adaptation of the Green-Lagrange strain tensor as:

$$\varepsilon_i = \frac{1}{2}\frac{l_i^2 - l_{i,0}^2}{l_{i,0}^2} \quad , \tag{1}$$

where l_i and $l_{i,0}$ are the current and origin lengths of the element.

Then the strain energy of the system, $\boldsymbol{U}$, can be given as:

$$U = \frac{1}{2}\sum_i D_i \varepsilon_i^2 \, , \tag{2}$$

where the stiffness coefficient is defined as $D_i = E_i A_i l_i$, $E_i A_i$ is the extension's stiffness of bar i.

Strain energy is the functional of the strain. Considering the stationary conditions for the strain energy, i.e. the variation of the function equals to zero, leads to:

$$\frac{\delta U}{\delta \varepsilon_i} = \sum_i D_i \varepsilon_i \delta q_i = 0 \, , \tag{3}$$

where q is the nodal coordinates.

Then the kinematic of the system can be described as:

$$\begin{cases} \delta U = 0; \\ \Phi(q,t) = 0, \end{cases}, \tag{4}$$

where $\boldsymbol{\Phi}(q, t)$ is the constraint equation of the system.

To solve the kinematic problem Eq. (4), a set of Lagrange multipliers λ will be introduced to put the problem in the equivalent unconstrained matrix form as:

$$f(\boldsymbol{U}, \boldsymbol{\Phi}) = \frac{1}{2}\boldsymbol{\varepsilon}^T(\boldsymbol{q})\boldsymbol{D}\boldsymbol{\varepsilon}(\boldsymbol{q}) + \boldsymbol{\lambda}^T\boldsymbol{\Phi}(\boldsymbol{q},t), \tag{5}$$

where $\boldsymbol{D}$ is the kernel stiffness matrix as diag($E_i A_i l_i$).

The stationary of the above functional generate the variation equations as:

$$\begin{cases} \delta \boldsymbol{q}^T \left[\boldsymbol{E}^T(\boldsymbol{q})\boldsymbol{D}\boldsymbol{\varepsilon}(\boldsymbol{q}) + \boldsymbol{B}^T(\boldsymbol{q})\boldsymbol{\lambda} \right] = 0; \\ \delta \boldsymbol{\lambda} \boldsymbol{\Phi}^T(\boldsymbol{q}) = 0, \end{cases} \tag{6}$$

where $\boldsymbol{E}$ and $\boldsymbol{B}$ are the strain matrix and Jacobian matrix of the constraints given as: $\boldsymbol{E} = \dfrac{\delta \boldsymbol{\varepsilon}}{\delta \boldsymbol{q}}$ and $\boldsymbol{B} = \dfrac{\delta \boldsymbol{\Phi}}{\delta \boldsymbol{q}}$.

Taking account of the arbitrariness of the virtual displacement provides then the set of nonlinear equations become as:

$$\begin{cases} \boldsymbol{E}^T(\boldsymbol{q})\boldsymbol{D}\boldsymbol{\varepsilon}(\boldsymbol{q}) + \boldsymbol{B}^T(\boldsymbol{q})\boldsymbol{\lambda} = 0; \\ \boldsymbol{\Phi}(\boldsymbol{q}) = 0. \end{cases} \tag{7}$$

Then the dynamic equation can be obtained with the Hamilton's principle as [20]:

$$\begin{cases} \boldsymbol{M}\ddot{\boldsymbol{q}}(t) + \boldsymbol{E}^T(\boldsymbol{q})\boldsymbol{D}\boldsymbol{\varepsilon}(\boldsymbol{q}) - \boldsymbol{F}^T + \boldsymbol{B}^T(\boldsymbol{q},t)\boldsymbol{\lambda} = 0; \\ \boldsymbol{\Phi}(\boldsymbol{q},t) = 0, \end{cases} \tag{8}$$

where $\boldsymbol{F}$ is the external load.

The finite element coordinates used above are absolute coordinates, and the total motion (rigid-body motion and elastic deformation) is directly referred to an inertial frame. Due to the large displacements and rotations of the mechanical elements with respect to this frame, the linear theory of elasticity is not applicable, and a nonlinear theory is necessary. An updated Lagrangian point of view can be used.

Let us suppose an approximate solution to Eq. (8) at time t is $\left(\ddot{\boldsymbol{q}}^*, \boldsymbol{q}^*, \lambda^*\right)$ and the exact solution at time t in the incremental form is $\boldsymbol{q} = \boldsymbol{q}^* + \Delta\boldsymbol{q}$, $\ddot{\boldsymbol{q}} = \ddot{\boldsymbol{q}}^* + \Delta\ddot{\boldsymbol{q}}$ $\boldsymbol{\lambda} = \boldsymbol{\lambda}^* + \Delta\boldsymbol{\lambda}$.

Then according the dynamic equation, the exact solution should satisfy:

$$\begin{aligned} &\boldsymbol{M}\left(\ddot{\boldsymbol{q}}^* + \Delta\ddot{\boldsymbol{q}}\right) + \boldsymbol{E}^T\left(\boldsymbol{q}^* + \Delta\boldsymbol{q}\right)\boldsymbol{D}\boldsymbol{\varepsilon}\left(\boldsymbol{q}^* + \Delta\boldsymbol{q}\right) - \\ &-\boldsymbol{F}^T + \boldsymbol{B}^T\left(\boldsymbol{q}^* + \Delta\boldsymbol{q}\right)\left(\boldsymbol{\lambda}^* + \Delta\boldsymbol{\lambda}\right) = \\ &= -\boldsymbol{r}\left(\ddot{\boldsymbol{q}}^* + \Delta\ddot{\boldsymbol{q}}, \boldsymbol{q}^* + \Delta\boldsymbol{q}, \boldsymbol{\lambda}^* + \Delta\boldsymbol{\lambda}\right) \end{aligned} \tag{10}$$

and

$$\boldsymbol{\Phi}\left(\boldsymbol{q}^* + \Delta\boldsymbol{q}\right) = 0 \, , \tag{11}$$

where $\boldsymbol{r}$ is the residual vector, which indicates the unbalanced force of the system.

The Taylor expansion of the residual vector can be given as:

$$\begin{aligned} &\boldsymbol{r}\left(\ddot{\boldsymbol{q}}^* + \Delta\ddot{\boldsymbol{q}}, \boldsymbol{q}^* + \Delta\boldsymbol{q}, \boldsymbol{\lambda}^* + \Delta\boldsymbol{\lambda}\right) = \boldsymbol{r}^*\left(\ddot{\boldsymbol{q}}^*, \boldsymbol{q}^*, \boldsymbol{\lambda}^*\right) + \\ &+\boldsymbol{M}\Delta\boldsymbol{q} + \frac{\partial\left(\boldsymbol{E}^T\left(\boldsymbol{q}^*\right)\boldsymbol{D}\boldsymbol{\varepsilon}\left(\boldsymbol{q}^*\right)\right)}{\partial\boldsymbol{q}}\Delta\boldsymbol{q} + \frac{\partial\boldsymbol{B}^T\left(\boldsymbol{q}^*\right)}{\partial\boldsymbol{q}}\Delta\boldsymbol{\lambda} + \\ &\boldsymbol{B}^T\left(\boldsymbol{q}^*\right)\Delta\boldsymbol{\lambda} + o\left(\Delta\ddot{\boldsymbol{q}}^2, \Delta\boldsymbol{q}^2, \Delta\boldsymbol{\lambda}^2\right) = \boldsymbol{r}^*\left(\ddot{\boldsymbol{q}}^*, \boldsymbol{q}^*, \boldsymbol{\lambda}^*\right) + \\ &+\boldsymbol{M}\Delta\boldsymbol{q} + \boldsymbol{K}^T\Delta\boldsymbol{q} + \left[\boldsymbol{B}_2^T\left(\boldsymbol{q}^*\right) + \boldsymbol{B}^T\left(\boldsymbol{q}^*\right)\right]\Delta\boldsymbol{\lambda}, \end{aligned} \tag{12}$$

where $\boldsymbol{r}^*$ is the residual vector of the approximate solution, $\boldsymbol{K}$ is the stiffness matrix of the system and $\boldsymbol{B}_2$ is the second derivative of the constraint to the nodal coordinates, which can be given as:

$$\left.\begin{aligned} &\boldsymbol{r}^*\left(\ddot{\boldsymbol{q}}^*, \boldsymbol{q}^*, \boldsymbol{\lambda}^*\right) = \boldsymbol{M}\left(\ddot{\boldsymbol{q}}^*\right) + \boldsymbol{E}^{\mathrm{T}}\left(\boldsymbol{q}^*\right)\boldsymbol{D}\boldsymbol{\varepsilon}\left(\boldsymbol{q}^*\right) - \\ &-\boldsymbol{F}^{\mathrm{T}} + \boldsymbol{B}^{\mathrm{T}}\left(\boldsymbol{q}^*\right)\left(\boldsymbol{\lambda}^*\right); \\ &\boldsymbol{K}^{\mathrm{T}} = \frac{\partial\left(\boldsymbol{E}^{\mathrm{T}}\left(\boldsymbol{q}^*\right)\boldsymbol{D}\boldsymbol{\varepsilon}\left(\boldsymbol{q}^*\right)\right)}{\partial\boldsymbol{q}} \text{ and } \boldsymbol{B}_2^{\mathrm{T}} = \frac{\partial\boldsymbol{B}^{\mathrm{T}}\left(\boldsymbol{q}^*\right)}{\partial\boldsymbol{q}}. \end{aligned}\right\} \tag{13}$$

The Taylor expansion of the constraint equation is:

$$\begin{aligned} \boldsymbol{\Phi}\left(\boldsymbol{q}^* + \Delta\boldsymbol{q}\right) &= \boldsymbol{\Phi}\left(\boldsymbol{q}^*\right) + \frac{\partial\boldsymbol{\Phi}\left(\boldsymbol{q}^*\right)}{\partial\boldsymbol{q}}\Delta\boldsymbol{q} = \\ &= \boldsymbol{\Phi}\left(\boldsymbol{q}^*\right) + \boldsymbol{B}\left(\boldsymbol{q}^*\right)\Delta\boldsymbol{q} + o\left(\Delta\boldsymbol{q}^2\right). \end{aligned} \tag{14}$$

Thus, the above equations can be gathered in the single matrix equation as:

$$\begin{bmatrix} \boldsymbol{M} & \boldsymbol{0} \\ \boldsymbol{0} & \boldsymbol{0} \end{bmatrix}\begin{bmatrix} \Delta\ddot{\boldsymbol{q}} \\ \Delta\boldsymbol{q} \end{bmatrix}+\begin{bmatrix} \boldsymbol{K} & \boldsymbol{B}^T+\boldsymbol{B}_2^T \\ \boldsymbol{B} & \boldsymbol{0} \end{bmatrix}\begin{bmatrix} \Delta\boldsymbol{q} \\ \Delta\boldsymbol{\lambda} \end{bmatrix}= =\begin{bmatrix} -\boldsymbol{r}^*\left(\ddot{\boldsymbol{q}}^*,\boldsymbol{q}^*,\boldsymbol{\lambda}^*\right) \\ -\boldsymbol{\Phi}\left(\boldsymbol{q}^*\right) \end{bmatrix}. \quad (15)$$

The Newark's formula [23], which is widely used by structural engineers to solve problems of structural dynamics, is used in this paper to solve iteratively the dynamic Eq. (15).

3. Dynamic equations considering thermal effect

The effects of thermal loading on the mechanical behavior of structures have been studied and it shows the influence is significant [24-26]. Therefore, the movement of a multibody may be affected by the temperature changes. In this study, the temperature-dependent elastic modulus E is assumed to be constant over the cross section and along the longitudinal axis. This is because the temperature changes considered here are under 300℃. Under temperature change, the thermal strain at the axial line is:

$$\varepsilon_t=\alpha_t\Delta T, \quad (16)$$

where ΔT is the temperature increment relative to its ambient value and α_t is the coefficient of thermal expansion that is taken as 2.0×10^{-5}/℃ in this study.

The total strain of the bar can be described by:

$$\varepsilon=\varepsilon_e+\varepsilon_t, \quad (17)$$

where ε_e is the mechanical elastic strain and ε_t is the thermally induced strain. All the strains are defined as positive when acting in tension. Thus the mechanical strain ε_e of bar i can be given as:

$$\varepsilon_{ei}=\varepsilon_i-\varepsilon_{ti}=\frac{1}{2}\frac{l_i^2-l_{i,0}^2}{l_{i,0}^2}-\alpha_t\Delta T \quad . \quad (18)$$

Substituting Eq. (18) into Eq. (15) leads to the dynamic equations under external loads and temperature changes as:

$$\begin{bmatrix} \boldsymbol{M} & \boldsymbol{0} \\ \boldsymbol{0} & \boldsymbol{0} \end{bmatrix}\begin{bmatrix} \Delta\ddot{\boldsymbol{q}} \\ \Delta\boldsymbol{q} \end{bmatrix}+\begin{bmatrix} \boldsymbol{K} & \boldsymbol{B}^T+\boldsymbol{B}_2^T \\ \boldsymbol{B} & \boldsymbol{0} \end{bmatrix}\begin{bmatrix} \Delta\boldsymbol{q} \\ \Delta\boldsymbol{\lambda} \end{bmatrix}= =\begin{bmatrix} -\left(\boldsymbol{r}^*\left(\ddot{\boldsymbol{q}}^*,\boldsymbol{q}^*,\boldsymbol{\lambda}^*,T\right)+\boldsymbol{F}\left(\Delta T\right)\right) \\ -\boldsymbol{\Phi}\left(\boldsymbol{q}^*\right) \end{bmatrix}, \quad (19)$$

where T is the ambient temperature at time t, the residual vector can be written as:

$$\boldsymbol{r}^*\left(\ddot{\boldsymbol{q}}^*,\boldsymbol{q}^*,\boldsymbol{\lambda}^*,T\right)=\boldsymbol{M}\left(\ddot{\boldsymbol{q}}^*\right)+ +\boldsymbol{E}^T\left(\boldsymbol{q}^*,T\right)\boldsymbol{D}\boldsymbol{\varepsilon}\left(\boldsymbol{q}^*,T\right)-\boldsymbol{F}\left(\Delta T\right)+\boldsymbol{B}^T\left(\boldsymbol{q}^*\right)\left(\boldsymbol{\lambda}^*\right), \quad (20)$$

and $\boldsymbol{F}(\Delta T)$ is the nodal force induced by the temperature changes, which can be written as:

$$\boldsymbol{F}\left(\Delta T\right)=\boldsymbol{E}^T\left(\boldsymbol{q}^*,\Delta T\right)\boldsymbol{D}\boldsymbol{\varepsilon}_t\left(\Delta T\right). \quad (21)$$

4. Numerical examples

Numerical simulations are presented in this section in order to investigate the effect of thermal loading on the dynamic performances of deployable structures. A type of foldable truss system as shown in Fig. 1, which is based on based on the four-bar linkage, has been used for the retractable roof. Therefore, two numerical examples shown in Fig. 2, a general four-bar linkage and a parallel four-bar linkage, are used to compare the dynamic performances under different temperatures.

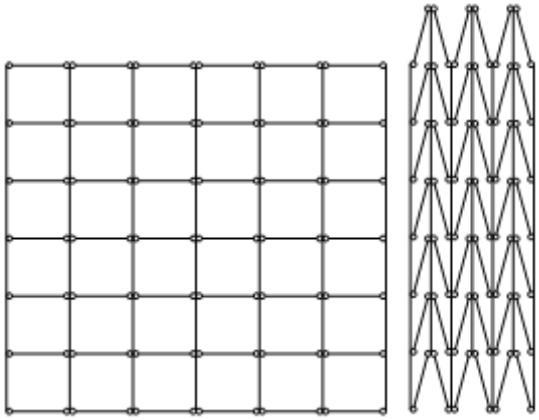

Fig. 1 Foldable truss structures

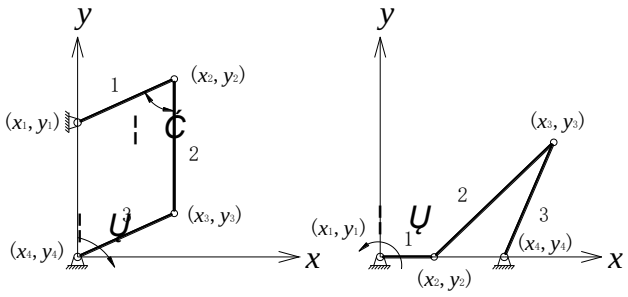

Fig. 2 Four-bar linkages: a - a parallel case, b - a general case

The two examples, whose material and geometric parameters are the same as those in Refs. [18] and [19], are given in Table 1, which shows the mass m, the elastic modulus E, the length l, the second moment of area I and the cross-sectional area A of the components. In this study, the lowest temperature is assumed to be about -150℃ and the highest is nearly +150℃. In order to investigate the effect of thermal loading on the motion of the mechanism, three cases in different temperature environments are established including the high temperature +150℃, the normal temperature 20℃ and the low temperature -150℃. Therefore, the temperature changes for these cases are:

$$\begin{cases} \Delta T_1=130°\text{C}, & \text{Case I : high temperature;} \\ \Delta T_2=0°\text{C}, & \text{Case II : normal temperature;} \\ \Delta T_3=-170°\text{C}, & \text{Case III : low temperature.} \end{cases} \quad (22)$$

Table 1

Geometry and Material Parameters of Four-bar Linkages

Linkage model	Element Number	E, MPa	A, m^2	m, kg	l, m
Parallel four-bar linkage	1	1.5×10^{11}	4.64×10^{-5}	0.288	0.288
	2	1.5×10^{11}	4.64×10^{-5}	0.357	0.357
	3	1.5×10^{11}	4.64×10^{-5}	0.288	0.288
General four-bar linkage	1	1.0×10^{9}	1.26×10^{-3}	0.6811	0.2
	2	5.0×10^{6}	1.96×10^{-3}	2.474	0.9
	3	5.0×10^{8}	7.07×10^{-4}	1.47	0.5197

It should be noted that the parallel four-bar linkage deploys with the initial angle $\gamma = 5°$, which will lead to avoid the bifurcation point of the motion path. In order to make the movement smoothly, bar 3 of the parallel four-bar linkage and bar 1 of the general four-bar linkage are driven following the specified motion planned by STEP function, the angle ω applied on driving bars is defined as follows:

$$\omega = \begin{cases} 0.365t^2(3-2t), & 0 \le t \le 1; \\ 0.365, & 1 \le t \le 4; \\ 0.365 - 0.365(t-4)^2(11-2t), & 4 \le t \le 5. \end{cases} \quad (23)$$

4.1. Results without thermal loading

Figs. 3 and 4 show the variation of element strains and nodal coordinates with time for parallel four-bar linkages and non-parallel four-bar linkages, respectively. It can be found from these figures that the change trend of element strains and nodal coordinates have the characteristic of symmetry for the parallel four-bar linkage. Moreover, the strains of every element have the same order of magnitude. However, for the non-parallel four-bar linkage, the difference of strains of every element is significant. This is because the elastic modulus of element 2 is smaller than other elements.

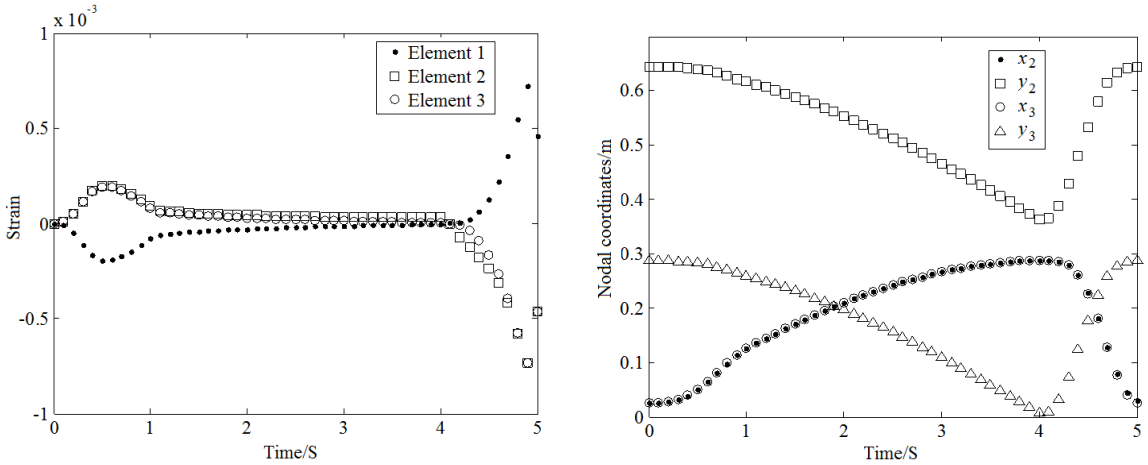

a b

Fig. 3 Results of parallel four-bar linkages: a - element strains; b - nodal coordinates

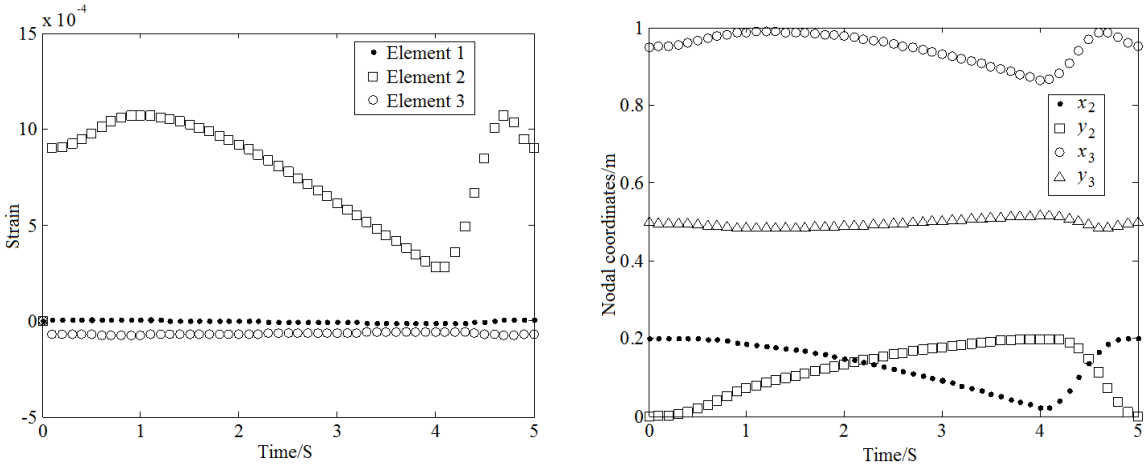

a b

Fig. 4 Results of non-parallel four-bar linkages: a - element strains; b - nodal coordinates

4.2. Results with thermal loading

The influence of thermal loading on the movement of four-bar linkages is shown in Fig. 5, which gives the strain variation of element 2 under different load cases. For the parallel four-bar linkage, it can be found the effect of temperature changes on the element strain is slight. However, the effect is significant for the non-parallel four-bar linkage. The element strain increases with the rise of the temperature during the most motion process. That is to say the thermal stress due to heat expansion will increase the constraint forces and the internal forces of bars. Moreover, the element strain also reduces with the decrease of the ambient temperature during the most motion process. It can also be found from results that the parallel four-bar linkage may be more suitable than the non-parallel four-bar linkage for retractable roof structures, because the influence of thermal effects is slight.

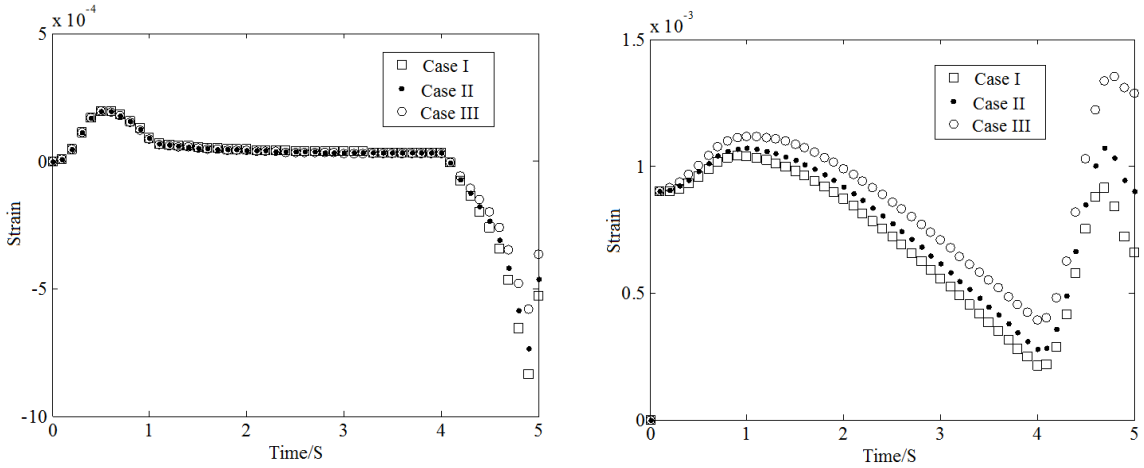

a b

Fig. 5 Effects of thermal loading: a - parallel four-bar linkages; b - non-parallel four-bar linkages

5. Conclusions

The thermal stress due to temperature rise may increase the element strain and internal forces. Moreover, this may induce the failure of the deployment of deployable structure. Therefore, it is necessary to discuss the flexible multibody systems under different thermal loading,. Based on this idea and formulation of finite element methods, the dynamic equations of the system considering the temperature effect are derived. Then two examples, a parallel four-bar linkage and a non-parallel four-bar linkage are presented in this paper to study the influence of thermal loading on the behavior during the motion.

In the present case, it was possible to omit taking into account bending deformation thanks to the 2D nature of the problem where hinge joints do not transit bending. For 3D problems, the need to consider rotations about arbitrary directions in space would be generally imply the introduction of bending strains also, which will be investigated in future. Another problem is to deal with the temperature effect of the cable structures including the air damping [27], which is very complex and difficult issue.

6. Acknowledgments

The work presented in this article was supported by the National Natural Science Foundation of China under Grant #51308106 and Grant #51578133, Specialized Research Fund for the Doctoral Program of Higher Education under Grant #20130092120018, a Project Funded by the Priority Academic Program Development of Jiangsu Higher Education Institutions, and the Excellent Young Teachers Program of Southeast University. Authors also thank the anonymous reviewers and the executive editor for their valuable comments and thoughtful suggestions which improved the quality of the presented work. A preliminary version of this article was presented at the ASME 2013 International Mechanical Engineering Congress & Exposition.

References

1. **Wang, T.; Xu, J.** 2015. Design and strength analysis of glass fiber-reinforced epoxy composite shelter, Mechanika 21(2): 107-111 http://dx.doi.org/10.5755/j01.mech.21.2.8624.
2. **Sokolowski, W.M.; Tan, S.C.** 2007. Advanced self-deployable structures for space applications, J. Spacecr. Rockets 44(4): 750-754. http://dx.doi.org/10.2514/1.22854.
3. **Zhou, W.; Chen, L.L.; Yu, H.J.; Peng, B.; Chen, Y.** 2016. Sensitivity jump of micro accelerometer induced by micro-fabrication defects of micro folded beams, Meas. Sci. Rev. 16(4): 228-234. http://dx.doi.org/10.1515/msr-2016-0028.
4. **Haug, E.** 1989. Computer-Aided Kinematics and Dynamics of Mechanical Systems, Prentice Hall College Div, 500p.
5. **Garcís de Jalón, J.; Bayo, E.** 1994. Kinematic and Dynamic Simulation of Multibody Systems, Springer-Verlag, 434p.
6. **Nikravesh, P.** 1988. Computer-Aided Analysis of Mechanical Systems, Prentice-Hall, 448p.
7. **Samin, J.C., Fisette, P.** 2003. Symbolic Modeling of Multibody Systems, Kluwer Academic Publishers, 476p.
8. **Shabana, A.** 1997. Flexible multibody dynamics: review of past and recent developments, Multibody Syst. Dyn. 1: 189-222. http://dx.doi.org/10.1023/A:1009773505418.

9. **Shabana, A.A.** 1996. Finite element incremental approach and exact rigid body inertia, J. Mech. Des. 118(2): 171-178. http://dx.doi.org/10.1115/1.2826866.
10. **Flanagan, D.P.; Taylor, L.M.** 1987. An accurate numerical algorithm for stress integration with finite rotations, Comput. Meth. Appl. Mech. Eng. 62: 305-320. http://dx.doi.org/10.1016/0045-7825(87)90065-X.
11. **Shabana, A.** 1998. Dynamics of Multibody Systems, Cambridge University Press, 2nd edition, 386p.
12. **Zhao, J.; Tian, Q.; Hu, H.Y.** 2013. Deployment dynamics of a simplified spinning IKAROS solar sail via absolute coordinate based method, Acta Mech. Sin. 29(1): 132-142. http://dx.doi.org/10.1007/s10409-013-0002-9.
13. **Mikkola, A.M.; Shabana, A.A.** 2003. Non-incremental finite element procedure for the analysis of large deformation of plates and shells in mechanical system applications, Multibody Syst. Dyn. 9(3): 283-309. http://dx.doi.org/10.1023/A:1022950912782.
14. **Dmitrodhenko, O.N.; Pogorelov, D.** 2003. Generalization of plate finite elements for absolute nodal coordinate formulation, Multibody Syst. Dyn. 10(1): 17-43. http://dx.doi.org/10.1023/A:1024553708730.
15. **Dufva, K.; Shabana, A.A.** 2005. Analysis of thin plate structures using the absolute nodal coordinate formulation, Proc. Inst. Mech Eng Pt K-J Multi-Body Dyn. 219(4): 345-355. http://dx.doi.org/10.1243/146441905X50678.
16. **Dmitrodhenko, O.; Mikkola, A.** 2008. Two simple triangular plate elements based on the absolute nodal coordinate formulation, J. Comput. Nonlinear Dynam. 3(4): 041012. http://dx.doi.org/10.1115/1.2960479.
17. **Shabana, A.A.; Yakoub R.Y.** 2001. Three dimensional absolute nodal coordinate formulations for beam elements: Theory, J. Mech. Des. 123(4): 606-613. http://dx.doi.org/10.1115/1.1410100.
18. **Shabana, A.A.** 2001. Definition of the elastic forces in the finite-element absolute nodal coordinate formulation and the floating frame of reference formulation, Multibody Syst. Dyn. 5(1): 21-54. http://dx.doi.org/10.1023/A:1026465001946.
19. **Li, T.J.; Wang, Y.** 2009. Deployment dynamic analysis of deployable antennas considering thermal effect, Aerosp. Sci. Technol. 13(4/5): 210-215. http://dx.doi.org/10.1016/j.ast.2009.04.005.
20. **Géradin, M.; Cardona, A.** 2000. Flexible Multibody Dynamics: A Finite Element Approach, John Wiley & Sons, New York, 340p.
21. **Brüls O.** 2005. Integrated simulation and reduced-order modeling of controlled flexible multibody systems, PhD thesis, Université de Liège, 256p.
22. **Lens, E.V.; Cardonda, A.; Géradin, M.** 2004. Energy preserving time integration for constrained multibody systems, Multibody Syst. Dyn. 11(1): 41-61. http://dx.doi.org/10.1023/B:MUBO.0000014901.06757.bb.
23. **Newmark, N.M.** 1959. A method of computation for structural dynamics, J. Eng. Mech. 85: 67-94.
24. **Chen, C.S.; Chen, W.R.; Lin, H.W.** 2016. Thermally induced stability and vibration of initially stressed laminated composite plates, Mechanika 22(1): 51-58. http://dx.doi.org/10.5755/j01.mech.22.1.8682.
25. **Cai, J.G.; Xu, Y.X.; Feng, J.; Zhang, J.** 2012. In-plane elastic buckling of shallow parabolic arches under an external load and temperature changes, J. Struct. Eng. 138(11): 1300-1309. http://dx.doi.org/10.1061/(ASCE)ST.1943-541X.0000570.
26. **Cai, J.G.; Feng, J.; Zhang, J.** 2012. Thermoelastic buckling of steel columns with load-dependent supports, Int. J. Non-Linear Mech. 47(4): 8-15. http://dx.doi.org/10.1016/j.ijnonlinmec.2012.03.004.
27. **Zhou, W.; Chen, Y.; Peng, B.; Yang, H.; Yu, H.J.; Liu, H.; He, X.P.** 2014. Air Damping Analysis in Comb Microaccelerometer, Adv. Mech. Eng., 373172, 6p. http://dx.doi.org/10.1155/2014/373172.

Jianguo Cai, Xiaowei Deng, Yaozong Zhao, Jian Feng

EFFECTS OF THERMAL LOADING ON THE DEPLOYMENT OF FOUR-BAR LINKAGES FOR RETRACTABLE ROOF STRUCTURES

S u m m a r y

The thermal stress due to temperature rise may increase the element strain and internal forces, which may lead to the failure of the deployment of deployable structure. However, few works are carried out to study the dynamic performance of the flexible multibody under different temperatures, especially for retractable roof structures. Based on this idea and formulation of finite element methods, the dynamic equations of the system considering the temperature effect are derived. Then two examples, a parallel four-bar linkage and a non-parallel four-bar linkage, are presented in this paper to study the influence of thermal loading on the structural behavior during the motion. The results show that the effect of temperature changes is slight for the parallel four-bar linkage, but the influence is significant for the non parallel four-bar linkage. It can be concluded that the former case may be more suitable for the deployable structures.

Keywords: temperature field; deployment; multibody dynamics; linkage; retractable roof.

Received June 23, 2015
Accepted April 14, 2017